UCRL-JC-110489
PREPRINT

# Light-Ion Spectroscopy With Exotic Targets

Gordon L. Struble and Robert G. Lanier
Lawrence Livermore National Laboratory

This paper was prepared for submittal to the
proceedings for the International Symposium on
Spectroscopy and Structure of Molecules and Nuclei,
Tallahassee, Florida
27 and 28 March 1992

June 30, 1992

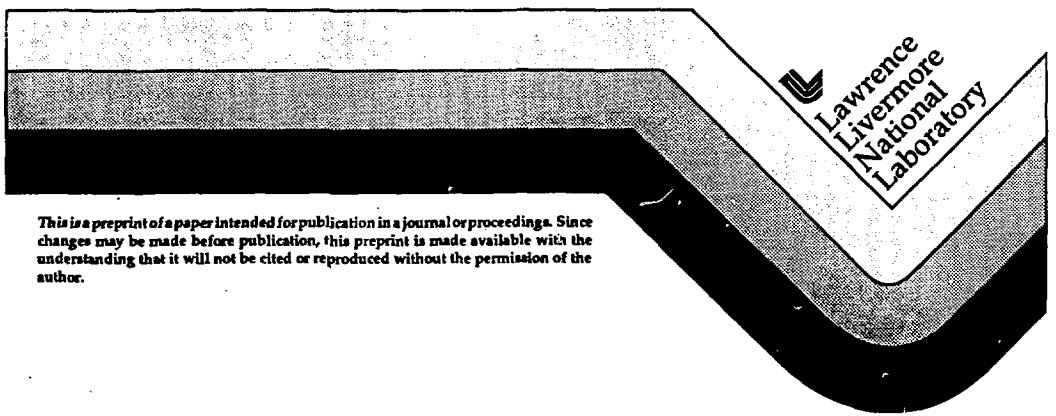

# LIGHT-ION SPECTROSCOPY WITH EXOTIC TARGETS

UCRL-JC--110489

DE92 017258

**GORDON L. STRUBLE**
*Lawrence Livermore National Laboratory, Livermore, California 94550*

and

**ROBERT G. LANIER**
*Lawrence Livermore National Laboratory, Livermore, California 94550*

## ABSTRACT

Understanding the rich and diverse aspects underlying the physics of nuclear structure requires a variety of experimental techniques. In our laboratory, we have concentrated on experimental techniques using light-ion probes and isotopes that are technically difficult to fabricate into targets. In particular, our studies of p-, d-, and t-induced nuclear reactions on the radioactive targets of $^{152,154}$Eu and $^{148}$Gd have illuminated some very specific and very interesting features of nuclear structure near the N = 89 shape-transition region.

## 1. Introduction

Over the past thirty years, nuclear spectroscopy has evolved and matured to the point that it is possible to determine much of the low-energy level structure of nuclei near the line of stability using neutrons and light and heavy ions as probes. However, even a complete catalogue of level energies may tell little about the interesting qualitative structural features of a nucleus. Instead, nuclear systematics and nuclear models can be used to develop intuitive insights about qualitative features of nuclear structure. These can then be tested and refined by studying very specific nuclear reactions that exhibit special selectivities.

With the many different and richly diverse aspects underlying nuclear structure, implementing a sensible program of study requires access to unique ion beams, specialized detectors, and unusual targets that may be very difficult to fabricate. The nuclear structure program at the Lawrence Livermore National Laboratory combines selected light-ion probes with targets of special nuclear materials to study specific and especially illuminating aspects of nuclear structure. In particular, our unique capabilities in chemistry, isotope separation, and handling of special nuclear materials have allowed us to make targets from materials that are rather difficult to purify and to handle. In Section 2 we will discuss in detail the construction of two such targets, $^{152}$Eu and $^{148}$Gd.

In Sections 3 and 4, we present some of the interesting nuclear spectroscopy and structure physics associated with these isotopes.

The details of the studies described here have been reported previously.[1–9] These articles contain citations of other associated work we have done as well as extensive reference lists relevant to the work described herein.

## 2. Special Targets for Nuclear Reaction Spectroscopy Studies

Although the idea of bringing together a focused particle beam and a stationary target is easy to conceptualize, in practice the preparation of a suitable target for an interesting physics experiment can be a formidable technical challenge. Many of our nuclear-related studies over the past several years have involved many interesting materials in the solid, liquid, and gaseous states. The most challenging studies have involved the use of radioactive materials as targets. In Table 1, we present a list of some of the special targets we have fabricated using various chemical purification techniques and isotope separation.

### *2.1. Preparation of the $^{152,154}$Eu Targets[1,2]*

Europium oxide enriched in either $^{151}$Eu or $^{153}$Eu from the Separated Isotopes Division at Oak Ridge National Laboratory was irradiated in the High Flux Isotope Reactor (HIFR) at Oak Ridge to form either $^{152}$Eu (13.5 y) or $^{154}$Eu (8.6 y). The irradiated material was shipped to our laboratory and placed in a remotely accessible hot cell where all subsequent chemical separation procedures were performed. The chemical procedures to separate the Sm and Gd activities were greatly simplified using a pressurized ion-exchange column. After chemical separation, the appropriate Eu activity was precipitated in the form of a quinolate and reduced in a tungsten crucible at 800 deg C to the oxide. This oxide material was then loaded into an isotope separator crucible and heated for an additional day to remove any sodium that would be present as

Table 1. Targets for nuclear studies prepared by the LLNL Nuclear Properties Group.

| Isotopic material | Half-life | Material production technique | Approximate thickness ($\mu g/cm^2$) |
|---|---|---|---|
| $^{148}$Gd | 75 y | Ta + p spallation | 25 |
| $^{151}$Sm | 90 y | $^{150}$Sm + n | 35 |
| $^{152}$Eu | 13 y | $^{151}$Eu + n | 30 |
| $^{154}$Eu | 8.6 y | $^{153}$Eu + n | 15 |
| $^{176}$Lu | — | — | 22 |
| $^{249}$Bk | 311 d | $^{247}$Bk + 2n | 30 |

a minor reagent contaminant because of the quinolate precipitation. Isotope separation began approximately 24 hr after the chemical separations were completed. Five usable targets containing approximately 1 μg each of radioactive Eu separated isotope were made in this way. Subsequent proton elastic scattering spectra from two selected targets showed Gd and Sm contaminations to be generally less than 1%.

### *2.2. Preparation of the $^{148}$Gd Target[2,3]*

The raw material for the $^{148}$Gd target was produced by spallation reactions in a Ta metal target by 750-MeV protons at the Isotopes Production Facility at LAMPF. Standard chemistries were used to separate the hafnium and lanthanide fractions at Los Alamos. The source material we obtained was the acidified lanthanide fraction, which became heavily contaminated with Pb during shipment. An initial assay of the material showed that it contained approximately 170 μg of $^{148}$Gd (75 y). We used standard ion-exchange chemistries to remove the Pb and rare-earth contaminants and obtained a clean Gd fraction that contained approximately 132 μg of $^{148}$Gd.

Samples for isotope separation were prepared by electrodeposition. The collector electrode was tungsten, and the material collected was very likely a form of hydrated gadolinium oxide. We collected material on eight such strips, which we estimated contained a total of 99 μg of $^{148}$Gd. These strips were placed in the isotope separator ion source, and sufficient material (about 1 μg) on each of four carbon substrates was collected. The four targets thus made contained a total of approximately 3–4 μg of $^{148}$Gd. The (p,t) reactions on one of these targets showed no evidence of contaminating peaks from other rare-earth elements.

The wet chemistry yields that we obtained could undoubtedly be improved. Also, the isotope separation yield experienced for the fabrication of this target is significantly less than what we experience for other rare-earth elements (30–70%). It is very likely that general procedures for fabricating such targets could be developed that begin with as little as 50 to 75 μg of desired radioactive isotope.

## 3. Shape Coexistence in the Isotopes of Eu

### *3.1. Deformation change at N = 89: Proton Inelastic Scattering at 12 MeV on $^{151,152,153,154}$Eu (Ref. 4)*

The europium isotopes in the region centered about A = 152 are of special interest because they apparently span an abrupt transition region. At N = 89, a change occurs in the ground state equilibrium shape and in other nuclear properties as well. These changes are experimentally well documented, and their abrupt nature is suggested by isotope-shift data on the europium nuclei between mass number 151 and 154. These data show that there is a strong increase in the mean-square nuclear-charge radius when one neutron is added to $^{151}$Eu.

For the odd-A europium isotopes centered about N = 89 (A = 151,153), the properties of the low-lying excited states have been well measured and extensively studied. Early Coulomb excitation experiments on $^{151}$Eu suggested that the low-energy structure could be interpreted as resulting from the coupling of a proton quasiparticle to a $2^+$ vibration. However, a subsequent calculation based on very similar assumptions was only partially successful. Attempts have been made to describe the low-lying structure of both $^{151}$Eu and $^{153}$Eu in terms of the Nilsson model by including the effects due to the Coriolis interaction. Assuming that $^{151}$Eu is a weakly deformed rotor, the calculations suggest that the ground state is the $2^+$ member of a severely distorted 3/2[411] rotational band. A similar calculation with $\beta \sim 0.32$ in $^{153}$Eu indicates that the general features of the 5/2[413] ground band and of other low-lying structures are fairly well reproduced. These Nilsson model calculations qualitatively explain some features of the two-nucleon transfer data and suggest that the model can be applied equally well across the Z = 63 transition region. The N = 89 species $^{152}$Eu has been the subject of intense experimental study. Available evidence suggests that probably all the low-lying levels can be interpreted in terms of two quasiparticles strongly coupled to a well deformed core and that the ground state can be interpreted as resulting from the antiparallel coupling of two Nilsson type orbitals: $\pi$3/2[411] and $\nu$11/2[505].

To further probe the nature of the shape transition in the region of europium nuclei, we have investigated the inelastic scattering of 12-MeV protons from isotopically enriched targets of $^{151,153}$Eu and from specially constructed $^{152}$Eu and $^{154}$Eu radioactive targets. We have also compared the data with the results of distorted wave-Born approximation (DWBA) and adiabatic coupled-channels (ACC) calculations.

The experiments were performed using a beam of 12-MeV protons from the EN-tandem accelerator stage of the Lawrence Livermore National Laboratory Cyclograaff facility. The elastic and inelastic proton groups were momentum analyzed in an Enge split-pole magnetic spectrometer. Angular distributions were measured for proton scattering on $^{152}$Eu, $^{153}$Eu, and $^{154}$Eu at 10-deg intervals beginning at 30 deg. The elastic cross sections used for normalization were obtained for $^{151}$Eu through a DWBA calculation. For $^{152,153}$Eu similar calculations were made using an ACC code.

A composite display shown in Figure 1 compares the proton spectra below ~600 keV observed at 130 deg for three nuclei. These data were obtained with the delay-line proportional counter mounted along the magnet focal plane and were plotted on the same energy scale to facilitate comparison. The spectra are intensity normalized so that the number of integrated counts in the elastic peak is the same for each spectrum.

The spin parity of the $^{152}$Eu ground state is $3^-$. The energy-level data are assigned rotational spin parities based on $3^-$ as a band head. The assignments are supported by the near constant rotational parameter of 11.2 keV, derived from the measured energy differences of adjacent states strongly populated in the (p,p') reaction. In $^{153}$Eu the measured rotational parameter is 12.0 keV and implies that the moment of inertia and hence the deformation is somewhat larger (~7%) for $^{152}$Eu. The data in Figure 1 strikingly exhibit the similarity of the (p,p') excitation of $^{152}$Eu and $^{153}$Eu and the corresponding dissimilarity of $^{151}$Eu. Because both $^{151}$Eu and $^{153}$Eu have the same

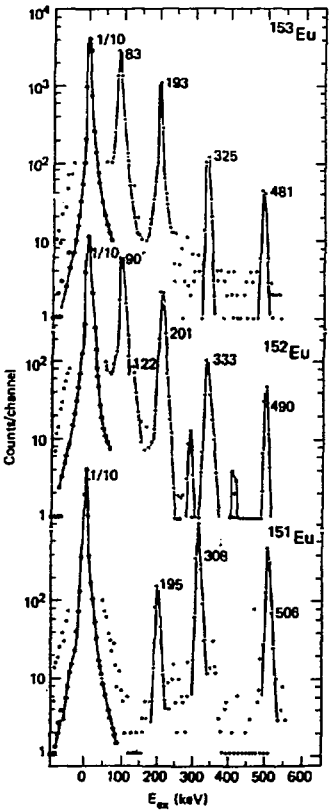


Figure 1. Proton scattering data at 12 MeV for $^{151}$Eu, $^{152}$Eu, and $^{153}$Eu. The 122-keV peak in the $^{152}$Eu spectrum is a result of accumulation of the $^{152}$Sm daughter.

ground-state spin parity $5/2^+$, the difference in their corresponding excitation patterns emphasizes the existence of the ground-state deformation change at $N = 89$.

The proton angular distributions measured for $^{152}$Eu, $^{153}$Eu, and $^{154}$Eu were compared with ACC and DWBA calculations. The use of ACC for inelastic scattering is a good approximation when the nucleus is well deformed and when the projectile energy is much larger than the rotational excitations. Also, making the calculation with ACC is advantageous because it includes all the rotational states of the excited band in the coupled-channels problem. Agreement between experiment and the ACC calculations for the deformed Eu nuclei shows that these nuclei both have rather large quadrupole deformations and measurable hexadecapole deformations. The deformation parameters are summarized in Table 2.

The scattering data measured from the $^{151}$Eu (p,p') reaction at 110, 120, and 130 deg were analyzed with a DWBA calculation. The nucleus was assumed to be a spherical harmonic vibrator, and the calculations were made using a complex collective model form factor. The optical model parameters were those used in the DWBA analysis of $^{152}$Eu and $^{153}$Eu. With this optical model set, the measured elastic cross sections are reproduced to within a few percent by the DWBA calculation. A simple average of our data gives $\beta = 0.13$. This result is somewhat smaller than $\beta$ values derived from B(E2) measurements for even-even vibrators isotonic with $^{151}$Eu: 0.190, $^{150}$Sm; 0.165, $^{152}$Gd. This suggests that the $^{151}$Eu levels strongly populated in the (p,p') reaction can be most simply interpreted as arising from simple $2^+$ core excitations.

The extremely well-behaved ground-state rotational structure in $^{152}$Eu is very probably due to the influence of the 11/2[505] Nilsson orbital in the intrinsic part of the ground-state wave function as is the fact that $^{154}$Eu has the same configuration for its ground state. These features may be qualitatively understood, considering that the total energy of the nucleus is obtained by summing the energies of the single particle orbitals. For nuclei with neutron numbers greater than $N = 82$, the nuclear potential-energy surface as a function of N becomes progressively softer because the extra core neutrons will tend to occupy downsloping orbitals. As the orbitals outside the core fill, the valence nucleons can gain energy by deforming. At some neutron number, this will eventually overcome the rigidity of the $N = 82$ core and the nucleus will deform.

The 11/2[505] orbital plays a particularly important role in the structure of nuclei near the $N = 89$ transition region. It is the most steeply rising orbital in this region, and it is also the $N = 82$ core orbital closest to the Fermi surface. Hole states involving the orbital are particularly interesting because they will involve promoting a particle from

Table 2. Summary of deformations derived from the proton inelastic scattering experiments.

| Nucleus | Calculation | $\beta_2$ | $\beta_4$ |
|---|---|---|---|
| $^{151}$Eu | DWBA | 0.13 | — |
| $^{152}$Eu | ACC | 0.28 | 0.06 |
| $^{153}$Eu | ACC | 0.28 | 0.06 |

this steeply upsloping orbital to one that is downsloping. The associated increase in single-particle energy can be compensated in part by a decrease in the energy of the total system through greater deformation. In such excitations, it is possible that the energy gained through deformation can compensate completely for the increase in single-particle energy so that the 11/2[505] orbital becomes the ground state. This apparently happens in the Eu nuclei at a deformation of $\beta_2 = 0.28$. Adding two more nucleons to $^{152}$Eu to form $^{154}$Eu involves a competition between filling the 11/2[505] orbital and filling the steeply downsloping 3/2[651] orbital, with a consequent increase in deformation. The latter alternative is more favorable; hence, the 11/2[505] orbital remains at the Fermi surface for N = 91.

The fact that the odd-odd nuclei are more rigid, as reflected by their rotational parameters, than $^{153}$Eu may be understood in terms of the resistance to deformation that is produced by nucleons that are confined to the steeply upsloping 11/2[505] orbital. For even N, the occupation probability of this orbital decreases with increasing deformation, while for odd N it remains constant (due to blocking) at a value of 0.5. Thus, the centrifugal force due to nuclear rotation will be less effective in producing deformation in the odd-N isotopes than it will in $^{153}$Eu, and the odd-N isotopes will therefore have greater rotational stability.

### *3.2. Evidence For a Strongly Deformed Prolate Shape at N = 87 from Two Nucleon Transfer Reactions on Targets of $^{152,154}$Eu (Ref. 5)*

The availability of isotopically enriched targets of $^{152}$Eu and $^{154}$Eu provided a new opportunity to study the spherical-deformed transition region along an unbroken sequence of the odd-Z Eu isotopes between N = 88 and N = 91. In this section, we present our data on two-nucleon transfer reactions on the odd-odd targets.

The particular specificity of the two-nucleon pick-up reaction provides compelling evidence for a strongly deformed {$\pi$5/2[413]; $\nu$11/2[505]}3$^-$ rotational band in $^{150}$Eu (N = 87). The (p,t) reactions were performed with 20-MeV protons at the Munich Technical University MP tandem van de Graaf facility, and the outgoing tritons were analyzed with a quadrupole-triple-dipole (Q3D) magnetic spectrograph. Angular distributions were measured in 10-deg increments between 10 deg and 50 deg. The shapes of the L = 0 transitions were calculated in DWBA, assuming pick up from the $(2f_{7/2})^2$ configuration. The calculated L = 0 angular distribution shapes are rather insensitive to the choice of configuration.

The $^{152}$Eu and $^{154}$Eu(p,t) reactions were repeated using an Enge split-pole spectrograph at the Lawrence Livermore National Laboratory Cyclograaff facility in order to measure more precise values for some of the absolute cross sections. A summary of the experimental data from all measurements is given in Figures 2 and 3 and Tables 3 and 4. Each spectrum in Figure 2 is a computer reconstruction from the original data such that (a) the ordinate scale is properly normalized to the differential cross section and (b) the abscissa is linear in energy. Moreover, to facilitate comparison of various features of

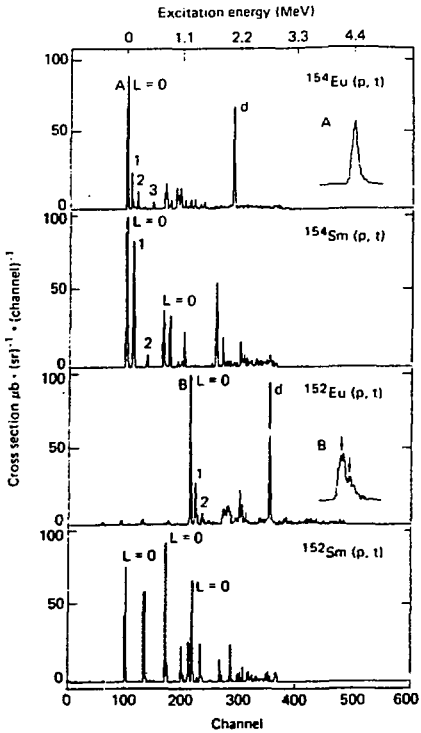


Figure 2. Triton spectra from the $^{154}$Eu, $^{154}$Sm, $^{152}$Eu, and $^{152}$Sm(p,t) reactions taken at 10 deg with the LLNL split-pole spectrograph. Insets A and B show the Munich high-resolution Q3D data for the lowest lying L = 0 transitions in the Eu nuclei. Rotational states corresponding to these band heads are numbered sequentially (1, 2, etc). The peaks labeled "d" in the Eu spectra result from small leakage through the grating electronics of the many deuteron signals from the $^{13}$C (p,d) reaction. In the Sm experiments, this deuteron interfering group was not focused on the counter.

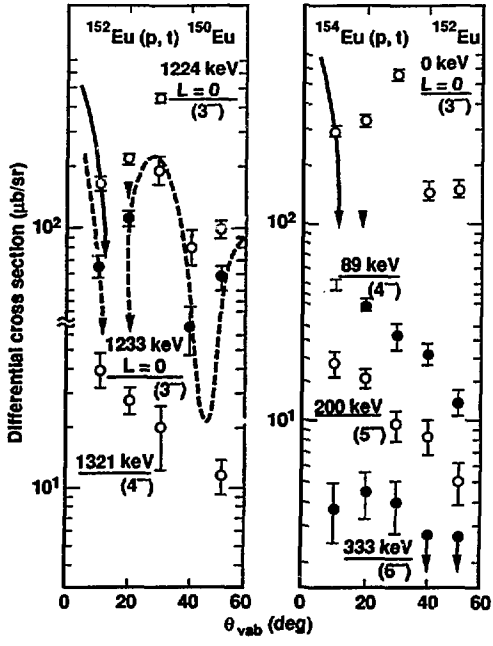


Figure 3. Angular distributions observed in the $^{152,154}$Eu(p,t) reactions (Munich Q3D data). The error bars represent only statistical uncertainties. The solid lines are DWBA calculations for L = 0 pickup from a pure $(2f_{7/2})^2$ configuration. The calculations are arbitrarily scaled to best fit the data. Calculations for other L-transfer values are not shown.

Table 3. Absolute differential cross section of L = 0 transitions observed in $^{154,152}$Eu and $^{154,152}$Sm(p,t) reactions (LLNL data). The quoted uncertainties represent statistical errors only.

| $\theta_{lab}$ (deg) | $\sigma(\theta)$ (μb/sr) | | | |
|---|---|---|---|---|
| | $^{150}$Eu[a] | $^{152}$Eu[b] | $^{150}$Sm[c] | $^{152}$Sm[d] |
| 10 | 228 ± 19 | 284 ± 25 | 392 ± 27 | 335 ± 19 |
| 20 | 350 ± 27 | 327 ± 26 | — | — |
| 30 | 588 ± 53 | 574 ± 59 | 1202 ± 58 | 841 ± 56 |
| sum[e] | 497 ± 43 | 491 ± 46 | — | — |

[a] Sum $\sigma(\theta)$ of for the 1224- and 1233-keV states.
[b] $\sigma(\theta)$ for the ground state.
[c] Sum of $\sigma(\theta)$ for the 0-, 738-, and 1255-keV states.
[d] Sum of $\sigma(\theta)$ for the 0- and 688-keV states.
[e] Sum = $2\pi \sum_{i=1}^{3} \sigma(\theta_i) \times \sin\theta_i \times (\Delta\theta)_i$.

Table 4. Relative intensity comparison at 10 deg for (p,t) population of states in $^{150}$Eu and $^{152}$Eu (Munich data).

| $^{150}$Eu | | $^{152}$Eu | |
|---|---|---|---|
| $E_x$[a] (keV) | $I_{Rel}$ | $E_x$ (keV) | $I_{Rel}$ |
| 1223.8 + 1232.8 | 1 | 0 | 1 |
| 1320.6 | 0.17 ± 0.01 | 89.0 | 0.17 ± 0.01 |
| 1438.0 | 0.04 ± 0.01 | 220.0 | 0.06 ± 0.01 |

[a] The relative excitation energies for strong peaks have an uncertainty of ±0.5 keV. The absolute uncertainty is about ±4 keV because of uncertainties in the Q values for the calibration reactions.

the data, the spectra have been shifted so that the centroids of the ground-state groups occur at the same channel position. In Figure 2, we note similar patterns of (p,t) excitations with targets of $^{152}$Eu and $^{154}$Eu. For the $^{154}$Eu(p,t) reaction, we observe strong L = 0 population of the ground state and progressively weaker excitation of the higher members of the {π5/2[413]; ν11/2[505]}3$^-$ ground-state band. Excited members of the band display featureless angular distributions.

The (p,t) excitation in $^{150}$Eu begins at 1224 keV with strong excitation of two very close-lying states with an intensity ratio (measured at 10 deg) of σ(1224 keV)/σ(1233 keV) ~ 2 (indicated by the arrows in inset B, Figure 2). Both states clearly show an L = 0 signature and are therefore 3$^-$ states. Moreover, the two states together account for virtually all of the L = 0 strength in the ground-state population of $^{152}$Eu observed by the $^{154}$Eu(p,t) reaction. This strong concentration of L = 0 strength in $^{150}$Eu implies that the 1224- and 1233-keV states have a large overlap with the deformed $^{152}$Eu ground state β ~ 0.28. Our data provide strong evidence for shape coexistence in $^{150}$Eu. If, for purposes of comparison, we ignore the doublet structure of the 1224- and 1233-keV peaks, then the relative intensities of the 1321- and 1438-keV states are in good agreement with those observed for the ground-state band seen in the $^{154}$Eu(p,t)$^{152}$Eu reaction. Moreover, the angular distribution of the 1321-keV state is featureless and very similar in character to that observed for the 89-keV state observed in $^{152}$Eu. Unfortunately, sufficient angular distribution data were not available for a similar comparison with the 1438-keV state.

Finally, in Figure 4, we show the systematic features of the {π5/2[413]; ν11/2[505]}3$^-$ bands in $^{152}$Eu, $^{154}$Eu, and $^{156}$Eu in comparison with the proposed rotational states in $^{150}$Eu. Assuming that the 1224-keV state is the band head, the trend suggests a smooth increase in rotational spacings with no evidence for a sharp discontinuity that might indicate a drastic shape difference. Thus, we conclude that there is a rotational band built on the {π5/2[413]; ν11/2[505]}3$^-$ configuration with a deformation of β ~ 0.28 and with its band head at 1224 keV. The obvious 3$^-$ doublet observed at 1228 keV is interesting but perhaps not surprising. At an excitation energy of 1.25 MeV, the predicted level density of 3$^-$ states is 0.1 per keV. Thus, a small residual interaction will mix the rotational state into the background of states with identical spin and parity. If the 1224-keV state were not strongly deformed, we would expect to see the

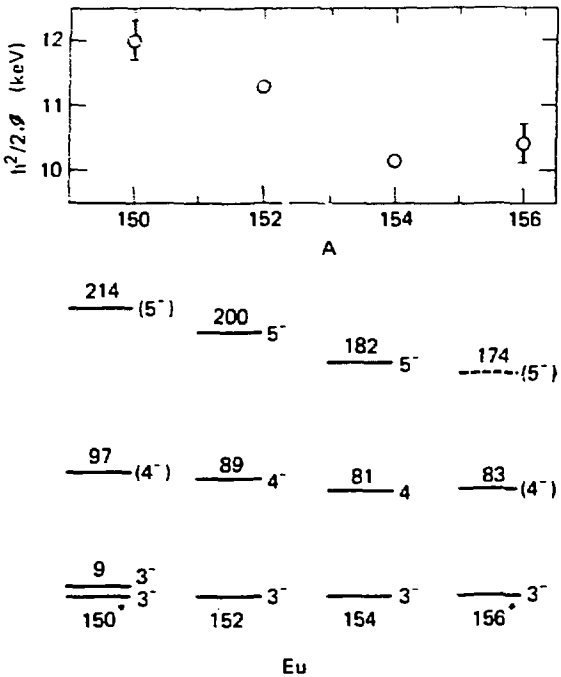


Figure 4. Rotational energy systematics and levels associated with the {π5/2[413]; ν11/2[505]}3⁻ configuration in $^{150,152,154,156}$Eu. The upper part shows values of the rotational parameter, $\hbar^2/2\mathcal{I}$, plotted against A. In the lower part, the asterisks indicate that an adjustment in the energy scale has been made to facilitate comparison. The band heads in $^{150}$Eu and $^{156}$Eu occur at 1224 keV and 461 keV, respectively.

L = 0 strength fragmented over a much larger range of excitation energy in analogy with the $^{152}$Sm(p,t)$^{150}$Sm reaction (see Figure 2).

The ground state of $^{150}$Eu is expected to be spherical, and our experimental data support this conclusion. From (p,t) Q-values, we can extract two-neutron separation energies. The systematics for the Eu isotopes show a distinct break at $^{150}$Eu. This break is associated with a shape change between $^{152}$Eu and $^{150}$Eu. These systematics will be discussed in more detail in a later section. Furthermore, we see no evidence for two-neutron pick-up strength below ~1.2 MeV. Our upper limit for cross sections of individual states below 1224 keV is 2 μb at 10 deg. Because two-nuclear transfer data between well-deformed odd-mass and odd-odd nuclei yield much larger cross sections,

even for non-favored transitions between intrinsic configurations, we conclude that there is an additional shape hindrance to states in $^{150}$Eu below ~1224 keV.

The presence of a strongly deformed $K^{\pi} = 3^-$ band in $^{150}$Eu is explained by blocking of the upward sloping 11/2[505] neutron orbital. As pointed out earlier, the effect of this orbital on deformation has been observed in $^{151}$Gd and $^{151}$Eu. A comparison of the gross features of the spectra in Figure 2 further suggests a stabilization of the deformation due to this blocking effect. In this figure, we plot the (p,t) spectra from two even-even Sm targets and the two odd-odd Eu targets. The latter have the 11/2[505] orbital as part of their ground-state configurations. The removal of two neutrons from $^{154}$Eu and $^{154}$Sm yields nuclei with ground states that are deformed, whereas a similar pair removal from $^{152}$Eu and $^{152}$Sm yields nuclei with essentially spherical ground states. In this regard, the interesting feature of the data in Figure 2 is that there is considerably more fragmentation of the (p,t) L = 0 strength in the two even-even targets than in the corresponding odd-odd targets. This suggests that the deformed even-even cores in the odd-odd systems are more rigid because there is less zero-point motion. Because the 11/2[505] orbital is so steeply upsloping, an odd particle in this orbital contributes a large specificity energy as the system changes shape adiabatically. Therefore, the amplitude of zero-point oscillations of configurations containing a quasiparticle in the orbital should be small. This is consistent with the experimental results in Figure 2.

We note in passing that the summed L = 0 strength for states below the pairing gap (~2 MeV) is larger for even-even nuclei than for odd-odd nuclei by about a factor of 2. This gap has been observed previously for odd-neutron superconducting systems and is attributed to a decrease in the pairing correlations because of blocking.

### *3.3. Evidence for Nuclear Shape Coexistence at N = 88 from Single Nucleon Transfer Reactions*[6,7]

Shape coexistence has been postulated for $^{151}$Eu. The earliest work involved measurements of Coulomb excitation and inelastic scattering, and these data were interpreted in terms of phonon excitations coupled to a $(d_{5/2})^{-1}$ ground state. States strongly populated in the ($^3$He,d) reaction suggested further spherical structures involving the $g_{7/2}$ and probably the $h_{11/2}$ proton (or proton holes) coupled to a $^{150}$Sm (or $^{152}$Gd) ground state. In (p,t) reaction studies, the states considered to have spherical structures were weakly populated and an additional set of states, starting with a $5/2^+$ level at 260 keV, were strongly populated. The authors postulated that this level is the band head of the 5/2[413] intrinsic Nilsson state. They also suggested that the level at 415 keV was a $7/2^+$ rotational band member and further interpreted levels at 654 and 801 keV as the $5/2^+$ and $7/2^+$ members of the β-vibrational band built on the 5/2[413] orbital. Subsequent in-beam gamma-ray experiments identified additional members of the deformed 5/2[413] band up to I = 11/2 and determined an average rotational parameter of 21.6 keV for the band. All of these experimental data are consistent with the notion that spherical and deformed structures coexist in $^{151}$Eu, and that inelastic scattering and the ($^3$He,d) reaction selectively populate spherical states, while the (p,t) reaction preferentially populates deformed states.

Although a spherical structure appears reasonable for the $^{151}$Eu ground state and for some of the higher-lying positive parity states, calculations suggest apparently conflicting possibilities. Calculations of the low-lying positive parity levels made by coupling single proton-hole motion in the $2d_{5/2}$ and $1g_{7/2}$ orbitals to the quadrupole vibrations of the $^{152}$Gd core found that the energy levels and B(E2) values reproduced reasonably well, but the calculated and experimental spin assignments of some of the levels did not agree. Subsequent experiments considerably improved the agreement with calculated results. However, problems such as the failure to predict the observed low-lying $3/2^+$ state at ~196 keV were apparent in the comparison. Moreover, the experimental data showed a decoupled band (~196 keV) built on the $h_{11/2}$ orbital. This band is consistent with expectations for a nucleus with a small deformation if Coriolis effects are included. Prompted by this observation, a Coriolis-mixing calculation was performed and attempts were made to describe the low-lying positive parity states and the states of the decoupled band in terms of mixtures of weakly deformed Nilsson states. By introducing different quadrupole deformations for the Nilsson orbitals derived from the $g_{7/2}$ ($\beta = 0.16$), $h_{11/2}$ ($\beta = 0.16$), and $d_{5/2}$($\beta = 0.11$) spherical states, a relatively consistent description was obtained of the $11/2^-$ decoupled band and of many features of the low-lying positive parity states. However, this model does not yield, for example, sufficient fragmentation of the B(E2) strength among the observed $3/2^+$ states and fails to account for the B(E2) value ($3 \times 10^{-4}$ $e^2b^2$) of the 260-keV "deformed" state by several orders of magnitude.

In view of the conflicting interpretations of the low-lying levels of $^{151}$Eu and the relation of these states to the question of shape coexistence, we performed (d,t) and (d,p) reaction studies on a target of $^{152}$Eu using a beam of 20-MeV deuterons from the three-stage tandem van de Graaff facility at the Los Alamos National Laboratory. We obtained energy spectra for the protons and tritons with a quadrupole-triple-dipole (Q3D) spectrograph. Triton spectra from the $^{152}$Eu(d,t) reaction were measured in 10 deg intervals between 15 and 65 deg. The spectra from the $^{152}$Eu(d,p) reaction were also taken in 10-deg steps, but the angular range was limited to between 25 and 65 deg. An independent check of the absolute cross-section determinations was performed at the Lawrence Livermore National Laboratory Cyclograaff facility using an Enge split-pole spectrograph.

Representative data from the $^{152}$Eu(d,t) and (d,p) runs are shown in Figures 5 and 6. The spectra are computer reconstructions from the original data so that the abscissas are linear in energy. Most of the charged-particle groups observed below 1 MeV are probably resolved singlets. Above this energy, the density of levels accessible by either a (d,p) or (d,t) reaction is high enough to preclude the resolution of individual states. For this reason, we have made no attempt to assign specific structures to any of these higher-lying states. A DWBA analysis of the angular distribution data was performed using the code DWUCK.

Inelastic scattering studies on $^{152,153}$Eu have demonstrated that the ground states of these transitional nuclei have both large deformations ($\beta = 0.3$) and very well-behaved ground-state rotational structures. The ground-state structures of both nuclei are also

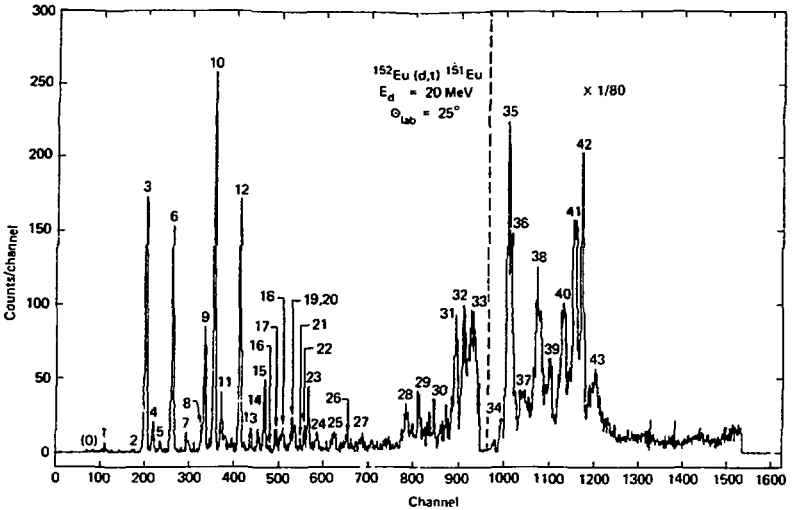


Figure 5. Experimental spectrum: $^{152}$Eu(d,t). The region to the right of the dashed line has been decreased by 1/80.

known: $^{152}$Eu, {π5/2[413]; ν11[505]}3$^-$ and $^{153}$Eu, π5/2[413]. The angular distributions of the (d,p) population of the 5/2[413] one-quasiparticle ground-state rotational band of $^{153}$Eu agree with the DWBA analysis when deformed Nilsson wave functions are used. The data exhibit an angular distribution consistent with a pure $\ell = 5$ signature, which virtually confirms the presence of the 11/2[505] neutron orbital in the two-quasiparticle ground state of $^{152}$Eu.

Above the ground band, the levels observed at 616 and 733 keV and the tentative level at 1400 keV show a single-particle strength of ~16% of the ground band. These levels account for the remainder of the observed single-particle strength below the energy gap. A majority of this remaining strength (~9%) is concentrated in the 616-keV level, which is also observed in Coulomb excitation experiments and is therefore probably a collective vibration with a small admixture of the π5/2[413] orbital. The nature of the remaining levels at 733 and 1400 keV cannot be determined from the present experiments.

The distribution of the $^{152}$Eu(d,p) single-particle strength below ~2 MeV can be understood in terms of structures that are characteristic of a strongly deformed nucleus. The spectrum virtually shows only these simple structures until one reaches an excitation

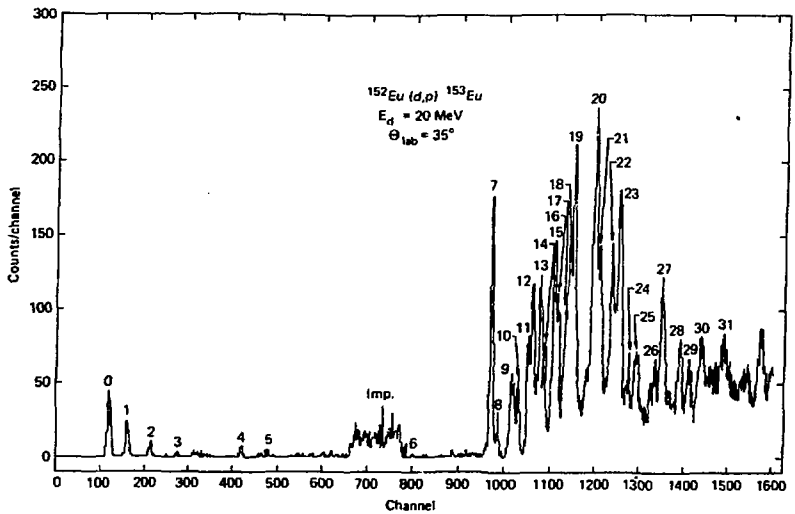


Figure 6. Experimental spectrum: $^{152}$Eu(d,p).

energy of ~2 MeV. Above this energy, the strength presumably results form the population of three-quasiparticle configurations, where the proton and one neutron are coupled to $\{\pi 5/2[413]; \nu 11[505]\}3^-$.

By contrast to the simple situation presented by the $^{152}$Eu(d,p) reaction, the spectrum from $^{152}$Eu(d,t) below ~2 MeV shows severe fragmentation of the single-particle pickup strength. Below ~2 MeV, there is almost complete correspondence between the levels populated in (d,t) and (p,t) although there are small relative differences in the degree of populating specific states. An earlier analysis suggested a description of the low-lying positive structures in $^{151}$Eu in terms of mixtures of weakly deformed Nilsson states. We now wish to consider this weakly deformed picture in light of the experimental data from the (d,t) reaction.

We have compared the experimental and calculated differential cross sections for the proposed deformed band in $^{151}$Eu at 260 keV. The cross sections were calculated assuming that the final-state configuration $\pi 5/2[413]$ and the calculated results were reduced by a factor of 3.2 to align them with the experimental data. The experimental angular distributions for the band members are consistent with a pure $\ell = 5$ signature. Figure 7 shows a comparison of the calculated and experimental intensities near the maximum of the $\ell = 5$ distribution. With the exception of the $11/2^+$ state, the angular

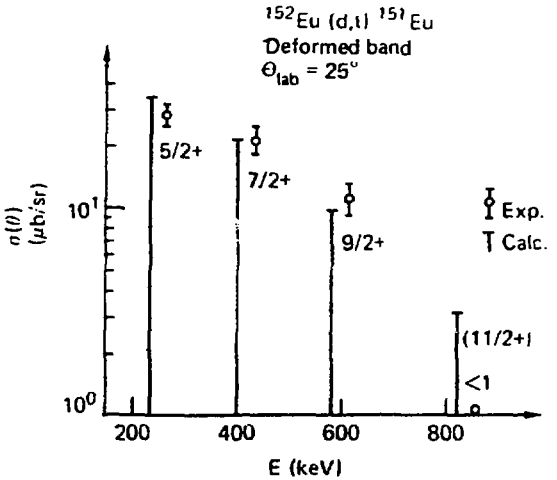


Figure 7. Comparison of the experimental and calculated (d,t) intensity patterns for the $5^+/2$, 260-keV deformed band in $^{151}$Eu.

distributions of the lower-lying levels and their predicted relative-intensity pattern are in excellent agreement with the data and are certainly suggestive of the assigned rotational character for these states. The fact that the full-strength (d,t) intensity appears hindered by a factor of 3 to 4 can be understood in terms of differences in the deformations of the target and residual states.

The ground and 22-keV states in $^{151}$Eu have spin parities of $5/2^+$ and $7/2^+$, respectively. Population of the ground state is not observed in our (d,t) studies, and the 22-keV state is only weakly populated. At a scattering angle of 25 deg, the 22-keV state has a measured cross section of 0.5 μb/sr, and the upper limit on population of the ground state is <0.09 μb/sr. The weakly deformed model posits that the levels near the ground state are weakly deformed ($\beta \sim 0.11$), and that the ground state is the $5/2^+$ member of a band built on the π3/2[411] Nilsson orbital, while the 22-keV state is primarily the $7/2^+$ member of a π7/2[404] band. The 5/2[413] band at 260 keV is also considered weakly deformed. It has a deformation ~45% larger (0.16) than the other lower-lying states and a factor of ~2 smaller than the measured deformation (~0.28) of the $^{152}$Eu ground state. A Coriolis-mixing calculation reproduces the low-lying level sequence of $^{151}$Eu reasonably well.

The wave functions derived from this calculation show that the ground state had a small (~2%) component of the 5/2[413] orbital, and that a much larger component (~30%) of this orbital is present in the 22-keV state. If we combine these admixtures with our predicted cross sections for a pure 5/2[413] configuration at 25 deg, we predict 2 and

21 μb/sr for the 0 and 22-keV states, respectively. When we combine the calculated cross sections with our experimental results, we estimate hindrance factors of >22 and 42, respectively, for population of these states with the (d,t) reaction. Recalling that the (d,t) hindrance from a target with $\beta = 0.28$ to the 260-keV band ($\beta = 0.16$) is only 3 to 4, it would seem that the nature of at least the 0- and 22-keV states ($\beta = 0.11$) significantly differs from that predicted weakly deformed picture. This analysis, and other measured properties of these states, strongly argues for their interpretation as nearly spherical structures.

The most striking feature of the $^{152}$Eu(d,t) spectrum is the extremely strong population of states in a narrow band of excitation energies between approximately 2.3 and 2.8 MeV. Virtually all the observed pickup strengths (~98%) are concentrated in these levels. Our hypothesis is that these states are strongly deformed ($\beta \sim 0.3$) and are essentially one-neutron holes coupled to the {π5/2[413]; ν11/2[505]}3$^-$ configuration, which is the ground state of $^{152}$Eu. The strongest support for this hypothesis would be the identification of individual rotational bands in this energy region. Unfortunately, the presence of a high density of states and the insufficient resolution of our experiments have made this virtually impossible. As a result, we have been able to look at only the gross properties of the spectrum for an interpretation of strongly deformed states. Our intent is to assume a deformed interpretation, compute the (d,t) spectrum, and compare the calculated results with the experimentally observed spectrum. A similar comparison will also be made for the (d,p) spectrum.

An immediate difficulty in reproducing the gross spectral properties of deformed levels with $E_{ex} > 2$ MeV is the uncertainty of the energy distribution of these states. Although energy distribution can be calculated in a deformed model, we have instead chosen a semiempirical approach because it is unclear that our conclusions would differ significantly if they are based on a more rigorous approach.

We decided to use the Nilsson single-particle states in our calculations based on experimental observations of states below ~1 MeV and (d,t) studies of the deformed N = 91 nucleus $^{155}$Gd. Because Nilsson model calculations suggest that other states are distributed among those observed in the stripping and pickup studies of $^{155}$Gd, we have also included some of these states in our tabulation. Those predicted "missing" states that would show strong population in (d,p) or (d,t) (e.g., 5/2[402]) were not included because they would have been observed if they contributed to structures below ~1 MeV. The remainder of the predicted states, which would be only weakly populated in stripping and pickup experiments, are included in our tabulation. This latter group of states is important because it forms part of the continuum on which the more strongly populated states rest. Generally, these weakly excited states would not be expected to markedly alter any strong detail present in the stripping or pickup spectrum, and, consequently, their energy uncertainty can be virtually ignored. We require only that some measure of their effect be included in the rather wide energy range we are considering. The single-particle energies of these "missing" states have been calculated in the Nilsson models. The quasiparticle energies of both the calculated and experimentally observed neutron states are estimated relative to the 3/2$^-$[521] orbital. Pairing factors relating to the neutron orbitals in the $^{152}$Eu target are derived from the one-quasiparticle energies, and the energies of the

three-quasiparticle residual states are calculated from the one-quasiparticle energies using $\Delta = 1.1$ MeV. The single-particle wave functions for all states have been taken from the Nilsson model calculation. Using the deformed neutron states associated with the N = 90 $^{155}$Gd core, we are implicitly assuming that within an interval of ~1 MeV the same states are also the main components of the deformed three-quasiparticle states coupled to what is now an N = 86 $^{151}$Eu core. If the N = 86 core associated with these states is in fact deformed, then this is a reasonable approximation. We do not expect, however, anything approaching detailed correspondence of the single-particle energies between either core.

The coupling of the odd-neutron quasiparticle to the two-quasiparticle configuration, which represents the $^{152}$Eu ground state, will split the single-particle strength into two bands separated by several tens of keV. To present a more realistic distribution of this splitting, we have used calculated splittings from the odd-odd nucleus $^{152}$Eu, which involve the 5/2[413] proton orbital and various neutron configurations. For orbitals not observed in $^{152}$Eu, we have arbitrarily assumed a splitting of 100 keV. The bands built on each configuration were assumed to have a constant value for the rotational parameter of 12 keV. On the basis of these assumptions, we have calculated the spectroscopic factors for each state of the various bands and used these spectroscopic factors along with the DWBA results to obtain predicted (d,t) and (d,p) cross sections. To partially account for configuration mixing, we distributed the cross section symmetrically about the calculated position of each state using an energy-dependent Lorentz factor. The experimentally observed and calculated (d,t) and (d,p) spectra are presented for comparison in Figure 8. The calculated spectral distribution for the $^{152}$Eu(d,t) reaction for E > 2 MeV shows very clearly that there is agreement with the general features of the experimental data. In particular, both the spectral intensity and its concentration in a rather narrow energy range can be accounted for. Although the individual and particular features of this region are not reproduced exactly, it is interesting to note that a count of the discrete peaks above any arbitrary intensity cutoff (say, 20% of the maximum intensity displayed by the strongest group) usually agrees with the experimental observations. In the $^{152}$Eu(d,p) reaction, one is confident that the states excited above ~2 MeV are, in fact, deformed. When we compare the experimental and calculated (d,p) spectra in Figure 8, our crude calculation again agrees reasonably well with experiment. In the calculated (d,p) spectrum, the strong pair of peaks that appear at ~3 MeV are a result of the 1/2[521] orbital. The experimental data on the Gd nuclei show that this orbital becomes lower in energy, relative to the 3/2[521] orbital for progressively larger mass numbers. For the three-quasiparticle states in $^{153}$Eu, if we had chosen single-particle states from $^{157}$Gd instead of $^{155}$Gd, the net effect would have been to move the levels from the 1/2[521] orbital more closely to the high-density region of the spectrum and thereby improve the agreement with the experimental (d,p) profile.

A comparison of the total spectral profile (0 to ~3 MeV) for both reactions shows an interesting contrast. The experimental (d,p) spectrum over the whole energy range looks much like the calculated profile. However, experimental (d,t) spectrum shows general agreement with $E_{ex} > 2$ MeV but is severely fragmented in the low-energy (<1.5 MeV) region.

Comparison of experimental data with our crude calculations suggests that the structures with $E_{ex} > 2$ MeV observed in $^{151}Eu$ can be reasonably interpreted as deformed three-quasiparticle states coupled to a core that has a deformation as large as the $^{152}Eu$ ground state. The presence of strongly deformed individual structures in $^{151}Eu$ would be interesting to isolate. Unfortunately, our experimental resolution was not adequate to separate cleanly any individual peaks above 2 MeV. The line structures noted in the lower half of Figure 8 represent the theoretical spectra before Lorentzian spreading. It is clear that there are a large number of closely packed states that would be difficult to resolve.

Our considerations of the gross properties of the high-energy (d,t) spectrum is not convincing proof that strongly deformed structures exist in $^{151}Eu$ above ~2 MeV. However, they are at least highly suggestive. On this basis, it would be interesting to test this hypothesis further with more quantitative calculations and higher resolution experiments.

### *3.4. Systematics of the Sm-Eu Transition Region*[8]

It has been known since 1956 that different nuclear shapes could exist in the same nucleus; more specifically, it was observed that the ground state of doubly magic $^{16}O$

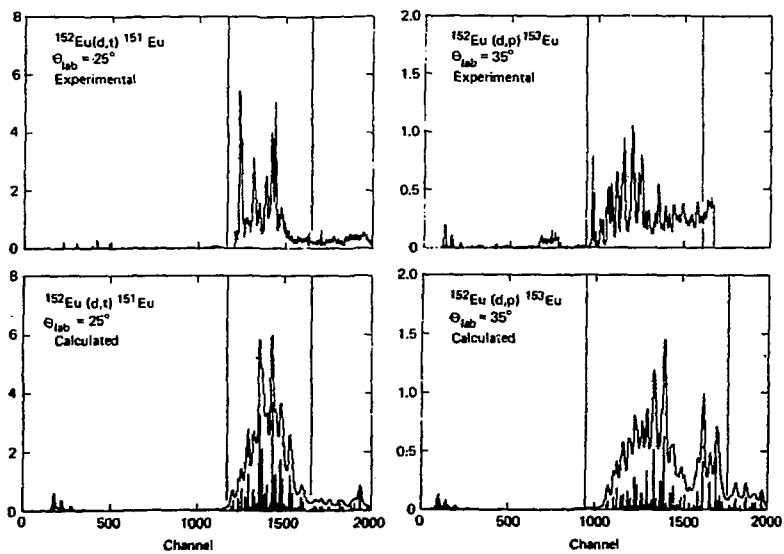


Figure 8. Comparison of the experimental and calculated (d,t) and (d,p) spectra from a $^{152}Eu$ target.

would be spherical, whereas the excited $0^+$ state at 6.05 MeV was the band head of a deformed rotational band. Several authors have suggested that even-even nuclei in the vicinity of N = 90 have both spherical and deformed states. Shape coexistence has also been suggested in several odd-A nuclei in this region. In particular, it is possible to follow the deformed 11/2[505] rotational band over a sequence of Sm, Gd, and Dy nuclei, which have an even number of protons and span the transition region between spherical and deformed nuclei. This fact is particularly apparent in the N = 87 nuclei $^{149}$Sm, $^{151}$Gd, and $^{153}$Dy, where many of the levels have at most only a small deformation. In the odd-A Eu nuclei, it is similarly possible to follow the systematics of the deformed 5/2[413] band from the strongly deformed region in $^{153,155}$Eu down to $^{151}$Eu, where the lowest-lying levels clearly do not represent deformed configurations. Finally, our various measurements of charged-particle reactions on radioactive targets of $^{152}$Eu and $^{154}$Eu have identified rotational states associated with the {$\pi$5/2[413]; $\nu$11/2[505]}$3^-$ configuration in the odd-odd Eu isotopes between $87 \leq N \leq 93$. These data demonstrate that coexistence of deformed and spherical states also exist in odd-proton nuclei and that this coexistence is associated with the 11/2[505] neutron orbital.

In Figures 9 and 10, we present the systematics for the two neutron separation energies, S(2n), as a function of neutron number. Figure 9 shows these systematics for the Sm isotopes, and Figure 10 shows them for the Eu isotopes. If we consider the simplest version of the liquid-drop mass formula, then we would expect a nearly linear change in the two-neutron binding energy as a function of neutron number. This result is expected because of the symmetry-energy potential term. Our plots of the ground-state separation energies show two discontinuities: one at N ~ 82 and the other at N ~ 88. The first is due to a major shell gap; the second is due to the onset of deformation. The interesting feature in both plots is that configurations involving a neutron quasiparticle in the 11/2[505] orbital do not exhibit a discontinuity at N ~ 88. From this, we assume that all such configurations are deformed and that nuclei such as $^{149}$Sm and $^{150}$Eu exhibit shape coexistence.

The 11/2[505] orbital is important in determining the shape of a nucleus because it is very steeply upsloping. Neutrons in this orbital resist deformation because their contribution to the total binding energy increases rapidly as the deformation increases. With one quasiparticle in this hole-like orbital, the orbital is only half occupied and the resistance to deformation is significantly reduced as compared to being fully occupied. This idea has been put in more rigorous form using microscopic Hartree-Bogoliubov calculations to study shape stability in (N = 87) $^{151}$Gd. These calculations yield both a stable and a strongly deformed nuclear structure whenever the 11/2[505] orbital is blocked.

The stabilizing role of the 11/2[505] orbital is emphasized by the plot of the rotational parameter versus the neutron number in Figure 11. From these data, we note that a rotational spacing persists deeper into the spherical region for both the odd-A and odd-odd systems, which involve states associated with this orbital. At N = 87, however, we observe that the 11/2[505] band in Sm, although still reasonably deformed, is beginning to show a strong departure from a smooth linear trace. We further note that this

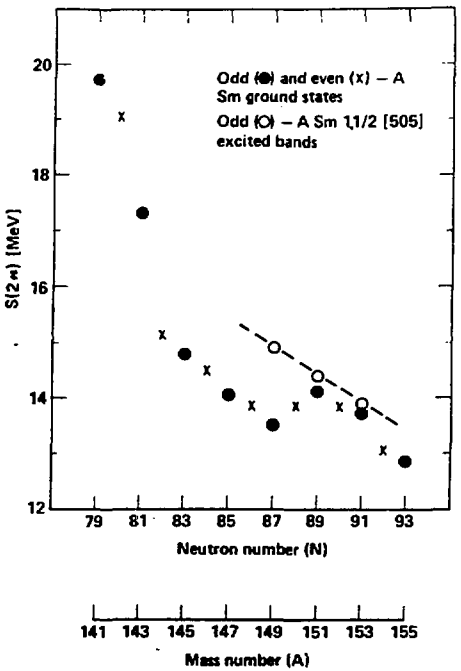


Figure 9. Two-neutron separation energies plotted vs N and A for a number of odd- and even-A Sm isotopes). Note the break in the systematics for ground-state bands in the region N ~ 86–90, and that there is no corresponding break in the systematics (dashed line) for the 11/2[505] deformed band.

effect is not observed for the $3^-$ states in the odd-odd Eu nuclei; the plot is virtually linear and rather flat in the range $87 \leq N \leq 93$. Such behavior for two-quasiparticle $3^-$ states is unexpected because the 5/2[413] orbital, which forms the proton component of these states, should provide little or no assistance to preserving deformation. This is suggested both by the systematics noted in Figure 5 for the lone orbital in the odd-A Eu nuclei and by the relatively flat deformation dependence of this orbital in a Nilsson diagram. Within the framework of the strong-coupling model, the only additional deformation stability achieved by the odd-odd Eu nuclei would be due to the residual interaction between the uncoupled neutron and proton. We have tested this possibility by evaluating the diagonal matrix elements for a reasonable residual interaction potential as a function of deformation and assuming the configuration $\{\pi 5/2[413]; \nu 11/2[505]\}3^-$. This term

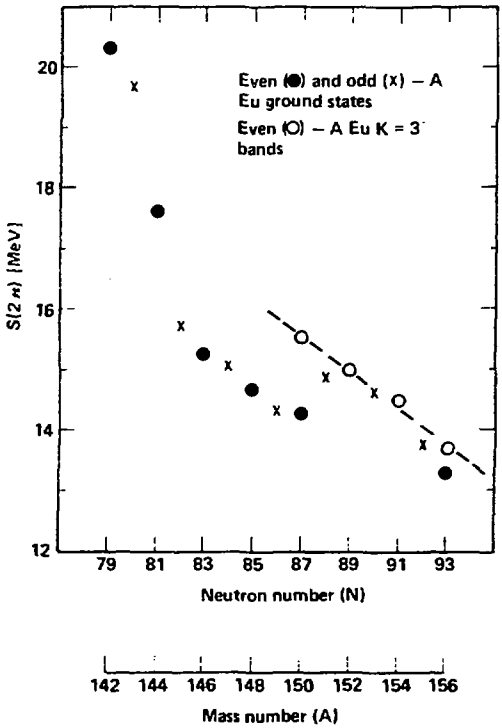


Figure 10. Two-neutron separation energies plotted vs N and A for a number of odd- and even-A Eu isotopes). Note the break in the systematics for ground-state bands in the region N ~ 86–90, and that there is no corresponding break in the systematics (dashed line) for the $K = 3^-$ states. The $K = 3^-$ states have the configuration {π5/2[413]; ν11/2[505]}, which forms the ground states of $^{152,154}$Eu and the excited states in $^{150,156}$Eu. The unusual similarity of these data with those shown in Figure 9 emphasizes the important role that blocking of the 11/2[505] orbital has on maintaining stable, deformed structures.

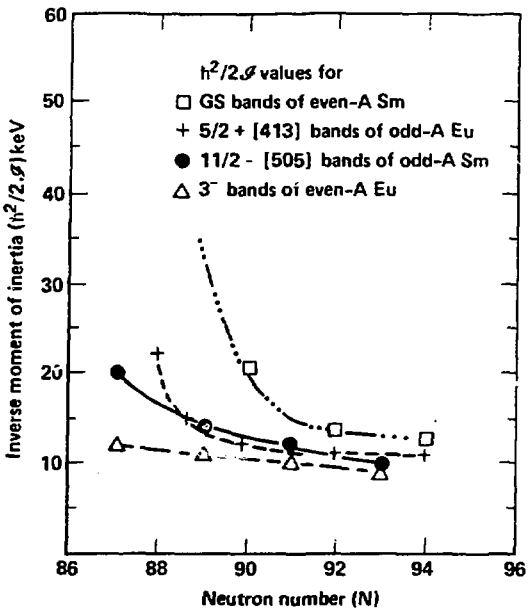


Figure 11. Inverse moments of inertia for different bands in Sm and Eu nuclei. Note that with a decreasing neutron number, the deformation of the $0^+$ ground-state bands of the even-even nuclei decreases dramatically first, followed by the 5/2[413] and 11/2[505] bands of the odd-A Eu and Sm, respectively. The $3^-$ bands of the odd-odd Eu nuclei show little tendency to decrease their deformation down to neutron number 87.

increases the binding energy as a function of increasing deformation, but only by ~30 keV between $\beta = 0$ and $\beta = 0.35$. Although the trend is correct, the magnitude of this effect is much too small to explain the behavior exhibited in Figure 11.

## 4. Pairing Vibrations in $^{146}$Gd

### *4.1. $^{148}$Gd(p,t) $^{146}$Gd Experiments*[3,9]

We carried out the $^{148}$Gd(p,t)$^{146}$Gd experiments at the Princeton University AVF Cyclotron facility. The proton-beam energy was 34.6 MeV in one set of experiments and 24.9 MeV in a later, less extensive run. Figure 12 presents triton-energy spectra observed with a Q3D spectrograph and obtained at 20 deg in the 34.6-MeV bombardments. The

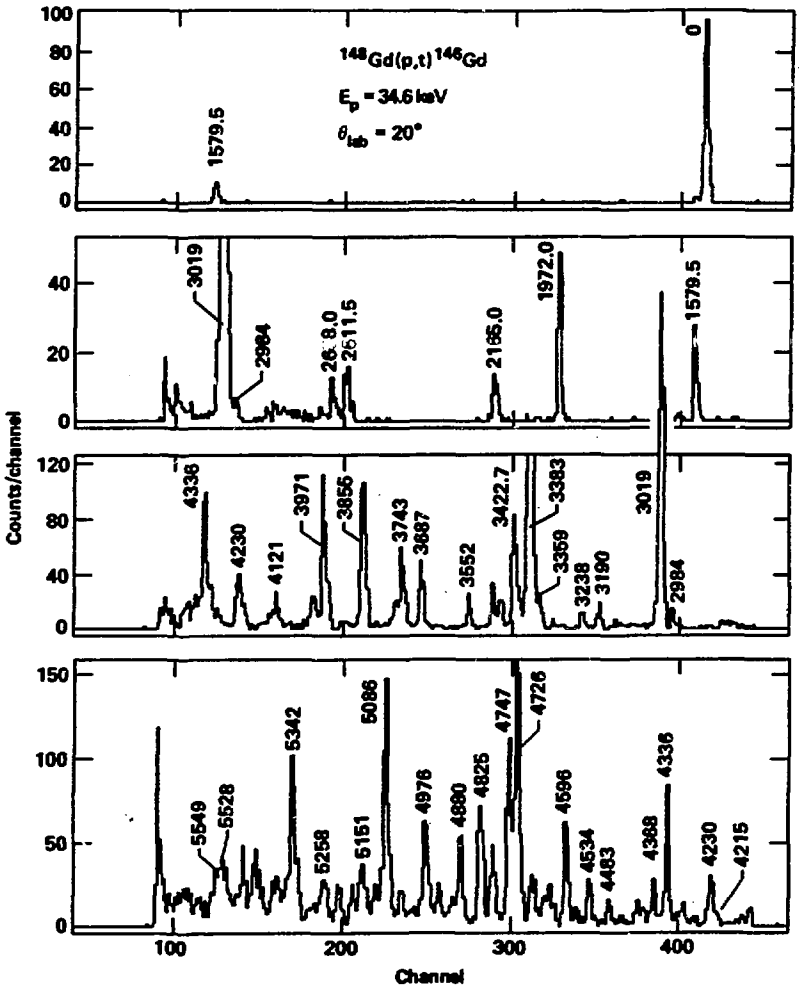


Figure 12. Triton spectra obtained with the Q3D spectrometer at $\theta_{lab} = 20$ deg for the $^{148}Gd(p,t)\ ^{146}Gd$ reaction. Selected peaks are labeled with their excitation energies obtained from $\gamma$-ray data to the nearest 0.1 keV or from the present work to the nearest keV.

spectra are shown from four different settings of the spectrometer, covering the range of excitation energies from 0 to 5.6 MeV in $^{146}$Gd.

The states that are populated most strongly in the (p,t) reaction are those formed by pickup of a correlated pair of neutrons. For a $^{148}$Gd target, these include the ground state and the neutron pairing vibration (pv) states in $^{146}$Gd. Other two-neutron states will be populated with various strengths, and we expect to see many of them in the region above 3.5 MeV of excitation. The states below 3.5 MeV are primarily two-proton configurations and therefore are only weakly populated. However, the $2_1^+$ and $3_1^+$ collective vibrational levels should be more strongly populated through their neutron 1p1h components. The first (p,t) experiments with these targets showed that most of the known states up to 3 MeV were populated with cross sections of a few microbarns or more.

Much of the (p,t) strength above 3.5 MeV should come from pickup of one valence neutron from the $f_{7/2}$ shell and one neutron from the filled orbitals below the N = 82 shell closure. In general, we cannot expect to identify specific configurations among the large number of experimental levels in this region. Our results follow earlier measurements. We see all the known states of natural parity below the 3290 keV state, except for those levels where the sensitivity is severely impaired because of closely spaced multiplets or proximity to the intense neutron (pv) peak at 3020 keV. At higher excitation energies, there is very little correspondence between the states we see (primarily two-neutron configurations) and the states identified in other reactions, which are primarily ($\alpha$,xn) that favor yrast states that are mostly proton configurations.

### *4.2. Comparison with the Harmonic-Pairing Vibration Model*

The doubly magic features indicated by the low-energy structure of $^{146}$Gd suggest that we should examine the strongly populated states at higher excitation energies in analogy to other doubly magic nuclei such as $^{208}$Pb. There is a wealth of two-nucleon transfer data for lead because several isotopes of Pb are on or near the line of stability and can be used as targets. These data show that there is strong evidence for the validity of the harmonic-pairing vibration model in the region near $^{208}$Pb.

The data on gadolinium will be much less extensive than for lead because $^{146}$Gd is far from the line of stability. However, it is interesting to show a comparison between selected low-lying levels in $^{142}$Sm with those seen at high excitation in $^{146}$Gd. Figure 13 shows the six most strongly populated low-lying states in $^{142}$Sm compared with selected high-lying states in $^{146}$Gd. The excitation-energy scales have been shifted to aid in the visual comparison of energy spacings by matching the 768-keV $^{142}$Sm level and the 3383-keV $^{146}$Gd level.

It is apparent from Figure 13 that there is good agreement between the energy spacings and cross sections of these four states in $^{142}$Sm and states we observe in $^{146}$Gd. However, the angular distribution data for the 5086- and 5258-keV peaks do not support this correlation. Although the (p,t) angular distributions may be anomalous for these two levels, similar ambiguities are not uncommon and may be resolved either by more accurate measurements or experiments that yield corroborating data.

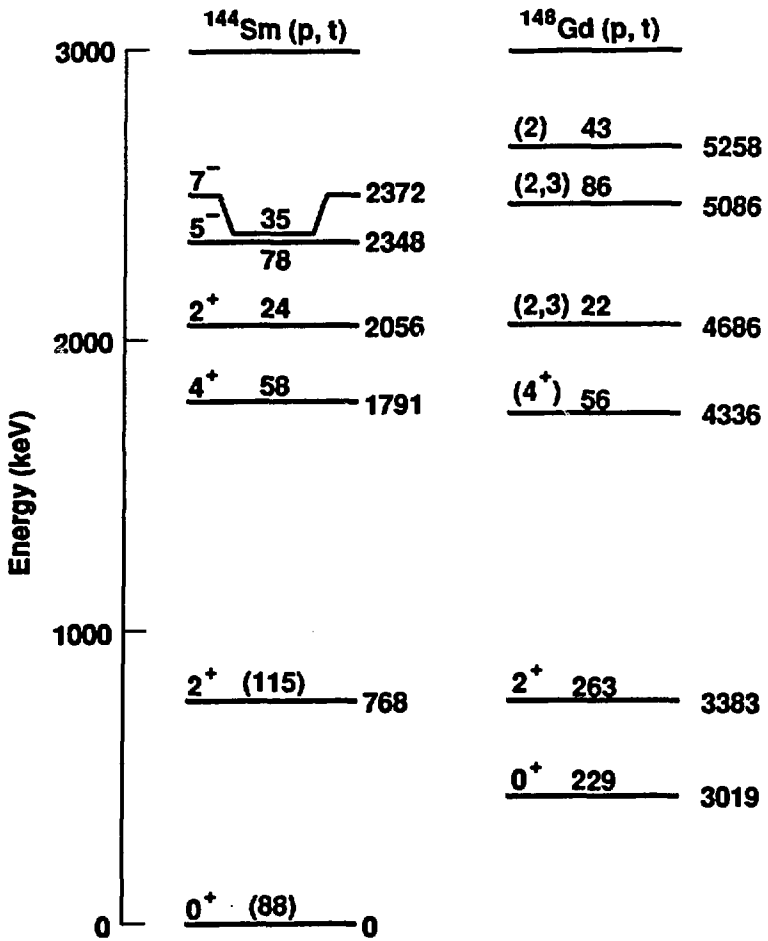


Figure 13. Comparison levels of $^{146}$Gd and $^{142}$Sm populated by the (p,t) reaction with 34.6-MeV protons. States are labeled with their $J^\pi$ values, excitation energies in keV, and (p,t) cross sections in μb. The energy scales have been shifted to facilitate the comparison of $^{146}$Gd levels in the pv region with low-lying $^{142}$Sm levels.

In summary, we have observed (p,t) population of many levels in $^{146}$Gd in the region between 0 and 5.5 MeV of excitation. Our results below about 3.5 MeV are in substantial agreement with those obtained from other studies. Most of the levels above 3.5 MeV are new, and many of them will be difficult to characterize because of their excitation energies. Finally, a comparison with the $^{144}$Sm(p,t)$^{142}$Sm reaction data shows a set of states in $^{146}$Gd that is in qualitative agreement with the harmonic-pairing vibrational model, supporting the doubly magic nature of $^{146}$Gd. However, certain details of the comparison show large deviations from this picture.

## 5. Conclusions

Using p-, d-, and t-induced reactions on radioactive targets of $^{152,154}$Eu and $^{148}$Gd, we have determined that the $h_{11/2}$ neutron orbital plays an important role in forcing a prolate shape for some of the low-lying states in the N = 89 Eu transition region. On the basis of proton inelastic studies, we have determined the magnitude of the ground-state deformation parameters for $^{151-154}$Eu. When we combined these data with other nuclear reaction studies, the states associated with the $h_{11/2}$ neutron orbital will very likely remain quite deformed down to N = 87. Our studies of single-nucleon transfer reactions with the $^{152,154}$Eu targets show in $^{151}$Eu the clear fragmentation of the deformed strength at near-ground state energies and the likely presence of stable deformed structures at several MeV. Using our data and other experimental data, we have shown that two-neutron separation energy systematics are linear with N and virtually identical for odd-A or odd-odd nuclear states that involve the 11/2[505] neutron quasiparticle. These systematics are in sharp contrast to the discontinous plot exhibited by the two-neutron separation energies for the even-proton Sm and the odd-proton Eu ground states.

Finally, our studies with the $^{148}$Gd target probed Z = 64, N = 82 shell closure by (p,t) tractions, which excite the pairing vibrations associated with closed shells. We obtain data that are in qualitative agreement with the harmonic-pairing vibration model and support a double closed-shell interpretation for $^{146}$Gd.

## 6. Acknowledgements

Work performed under the auspices of the U.S. Department of Energy by Lawrence Livermore National Laboratory under Contract W-7405-Eng-48.

## 7. References

1. R. J. Dupzyk, C. M. Henderson, W. M. Buckley, G. L. Struble, R. G. Lanier, and L. G. Mann, *Nucl. Instr. Methods* **153** (1978) 53.
2. R. G. Lanier, in *Nuclei of the Line of Stability*, eds. R. A. Meyer and D. S. Brenner (American Chemical Society, Washington DC, 1986).

3. L. G. Mann, R. G. Lanier, G. L. Struble, S. W. Yates, R. A. Naumann, and R. T. Kouzes, *Phys. Rev.* **C39** (1989) 2180.
4. R. G. Lanier, L. G. Mann, G. L. Struble, I. D. Proctor, and D. W. Heikkinen, *Phys. Rev.* **C18** (1978) 1609.
5. R. G. Lanier, G. L. Struble, L. G. Mann, W. Stoffl, I. C. Oelrich, J. Scheerer, I. D. Proctor, D. W. Heikkinen, and R. H. Howell *Phys. Letts.* **99B** (1981) 23.
6. G. L. Struble, I. C. Oelrich, J. B. Carlson, L. G. Mann, and R. G. Lanier, *Phys. Rev. Letts.* **39** (1977) 533.
7. R. G. Lanier, L. G. Mann, G. L. Struble, I. D. Proctor, and D. W. Heikkinen, *Phys. Rev.* **C22** (1980) 51.
8. R. G. Lanier, G. L. Struble, L. G. Mann, and J. A. Cizewski, *Nucl. Phys.* **A413** (1984) 236.
9. E. R. Flynn, J. van der Plicht, J. B. Wilhelmy, L. G. Mann, G. L. Struble, and R. G. Lanier, *Phys. Rev.* **C28** (1983) 97.